Patients with knee osteoarthritis can be divided into subgroups based on tibiofemoral joint kinematics of gait – an exploratory and dynamic radiostereometric study

Petersen, E. T.; Rytter, S.; Koppens, D.; Dalsgaard, J.; Hansen, T. B.; Larsen, N. E.; Andersen, M. S.; Stilling, M.

Published in:
Osteoarthritis and Cartilage

DOI (link to publication from Publisher):
10.1016/j.joca.2021.10.011

Publication date:
2022

Document Version
Publisher's PDF, also known as Version of record

Osteoarthritis and Cartilage 30 (2022) 249–259

Osteoarthritis and Cartilage

Patients with knee osteoarthritis can be divided into subgroups based on tibiofemoral joint kinematics of gait – an exploratory and dynamic radiostereometric study

E.T. Petersen † ‡ § *, S. Rytter ‖, D. Koppens † ‖, J. Dalsgaard †, T.B. Hansen † ‡, N.E. Larsen ¶ #, M.S. Andersen ††, M. Stilling ‡ § ‖

† *University Clinic for Hand, Hip and Knee Surgery, Holstebro Central Hospital, Lægårdvej 12 Holstebro, 7500, Denmark*
‡ *Department of Clinical Medicine, Aarhus University, Palle Juul-Jensens Boulevard 99 Aarhus N, 8200, Denmark*
§ *AutoRSA Research Group, Orthopaedic Research Unit, Aarhus University Hospital, Palle Juul-Jensens Boulevard 165 Aarhus N, 8200, Denmark*
‖ *Department of Orthopaedic Surgery, Aarhus University Hospital, Palle Juul-Jensens Boulevard 165 Aarhus N, 8200, Denmark*
¶ *Department of Radiology, Holstebro Central Hospital, Lægårdvej 12 Holstebro, 7500, Denmark*
# *Department of Radiology, Aarhus University, Palle Juul-Jensens Boulevard 99 Aarhus N, 8200, Denmark*
†† *Department of Materials and Production, Aalborg University, Fibigerstræde 16 Aalborg, 9220, Denmark*

ARTICLE INFO

Article history:
Received 30 June 2021
Accepted 23 October 2021

Keywords:
Knee osteoarthritis
Radiostereometry
Kinematics
Gait analysis
Clustering
Statistical parametric mapping

SUMMARY

Objective: Patients with advanced knee osteoarthritis (KOA) frequently alter their gait patterns in an attempt to alleviate symptoms. Understanding the underlying pathomechanics and identifying KOA phenotypes are essential to improve treatments. We investigated kinematics in patients with KOA to identify subgroups of homogeneous knee joint kinematics.

Method: A total of 66 patients with symptomatic KOA scheduled for total knee arthroplasty and 15 age-matched healthy volunteers with asymptomatic, non-arthritic knees were included. We used k-means clustering to divide patients into subgroups based on dynamic radiostereometry-assessed tibiofemoral joint kinematics. Clinical characteristics such as knee ligament lesions and KOA scores were graded by magnetic resonance imaging and radiographs, respectively.

Results: We identified four clusters that were supported by clinical characteristics. *The flexion group* ($n = 20$) consisted primarily of patients with medial KOA. *The abduction group* ($n = 17$) consisted primarily of patients with lateral KOA. *The anterior draw* group ($n = 10$) was composed of patients with medial KOA, some degree of anterior cruciate ligament lesion and the highest KOA score. *The external rotation* group ($n = 19$) primarily included patients with medial collateral and posterior cruciate ligament lesions.

Conclusion: Based on tibiofemoral gait patterns, patients with advanced KOA can be divided into four subgroups with specific clinical characteristics and different KOA-affected compartments. The findings add to our understanding of how knee kinematics may affect the patient's development of different types of KOA. This may inspire improved and more patient-specific treatment strategies in the future.

Introduction

Knee osteoarthritis (KOA) is commonly associated with pain, stiffness, muscle weakness, and joint instability. Thus gait and movement patterns are affected limiting daily activities[1]. Joint pathomechanics in KOA are complex and may affect the entire gait cycle. Even so, most studies have investigated the kinematics in KOA using observer-selected outcomes, i.e., individual discrete time-points, excursion, maximum, and minimum. The entire kinematic trajectory in patients with KOA has never been studied using non-directed hypothesis testing such as statistical parametric mapping (SPM) preventing selection bias[2,3]. This may potentially contribute with patient-specific characteristics of importance for rehabilitation and surgical results.

* Address correspondence and reprint requests to: E. T. Petersen, MSc., Orthopeadic Research Unit Aarhus University Hospital, Palle Juul-Jensens Boulevard 165, J501 Aarhus N, 8200, Denmark. Tel.: 45-22-88-88-60.
E-mail address: emiltp@clin.au.dk (E.T. Petersen).

https://doi.org/10.1016/j.joca.2021.10.011

Classically, kinematic changes in KOA have been reported as comparisons of group categories such as KOA severity[4–6], affected knee compartment[7], anterior cruciate ligament (ACL) deficiency[8], and walking difficulties[9]. However, such predefined categories may promote unnecessary bias and blur kinematic differences due to other unidentified characteristics. A reverse approach may allocate patients with KOA into subgroups based on homogenous kinematic gait trajectories and identify multiple characteristics that affect the kinematic motion patterns between groups. K-means is a centroid-based clustering algorithm using an unsupervised machine-learning approach that previously has been applied on kinematic trajectories[10]. Without prior knowledge of patient or disease characteristics, the algorithm allocates multidimensional data into homogenous subgroups based on an Euclidean distance measure.

Measurement of small kinematic differences requires precise methods. Dynamic radiostereometry (dRSA) can register the three-dimensional bone-pose and accurately measure small kinematic changes in native knees with ligament lesions and reconstructions[7,11–13].

In the present study, we investigated the full-trajectory knee joint kinematics during level gait in patients with advanced KOA to identify: 1) subgroups of KOA patients based on knee kinematics through clustering, and 2) features of knee kinematics unique to the identified subgroup, linking kinematics to patient characteristics describing the subgroup. We compared the results with data from a group of healthy volunteers with asymptomatic non-arthritic knees.

Methods

This study involved the preoperative data of 81 subjects (Table I) who participated in a randomized controlled study investigating the outcome of knee arthroplasty designs (ClinicalTrials NCT03633201). The inclusion period was from 2017 to 2019. A total of 66 patients with radiographic and symptomatic primary KOA were included. The control group comprised 15 local healthy, age-similar volunteers with asymptomatic knees and no radiographic KOA. The inclusion and exclusion criteria are presented in Table II. The study was approved by the Committee on Biomedical Research Ethics of the Central Denmark Region (1-10-72-303-16, issued 28 February 2017) and registered with the Danish Data Protection Agency (1-16-02-582-16, issued 31 October 2016). The study was conducted in accordance with the Helsinki Declaration, and written informed consent was obtained from all participants. The total estimated effective dose exposed to each patient was 0.629 mSv.

Experimental protocol

Participants walked barefoot on a leveled treadmill (Sole F63, Jonesboro, AR, USA) to mimic level gait (Fig. 1). They had a habituation period to get familiar with the test environment, with slowly increasing speed reaching a final speed of 0.83 m/s. This is slightly slower than average walking speed (1.25 m/s)[14] and was chosen to avoid exclusion of gait-disabled patients and facilitate sufficient dRSA data generation throughout the entire gait cycle. When the subject felt comfortable, data collection was initiated. Up to seven coherent gait cycles were obtained. For precaution and anticipating loss of balance during testing, subjects had a rail they could hold on to. Only none-rail-supported gait trials were included for further analysis. An overview of the workflow is illustrated in Fig. 2.

Dynamic radiographic imaging

The gait trials were recorded with a dedicated dRSA system (AdoraRSA; NRT X-Ray A/S, Hasselager, Denmark) with a previously described biplanar setup[13]. The radiation exposure parameters were set at 90 kVp, 600 mA, and a pulse-width of 2.5 ms, utilizing the highest frame rate of 15 Hz without compromising the image size. Simultaneously with the dRSA system, we used a minimum of six OptiTrack Prime 13 motion cameras (NaturalPoint, Corvalis, OR, USA) and Motive software (Motive v.2.0.0, NaturalPoint, USA) to assess the trajectories of skin-attached reflective markers (diameter: 10 mm). Prior to usage, the entire recording area was calibrated using an OptiTrack CW-500 Calibration Wand (NaturalPoint, USA). A custom-programmed Raspberry Pi 3 Model B (Linux Mini PC, Broadcom BCM2837 1.2 GHz Quad-Core 64-bit, 1 Gb LPDDR2 RAM) was used to time-synchronize data from the dRSA and the optical marker systems using pulse information from both systems.

	Patient group	Healthy control group
Inclusion criteria	Age above 18 years but no more than 80 years of age. Informed and written consent. Primary knee osteoarthritis in capable men and women. Indication for cruciate-retaining total knee arthroplasty.	Age above 18 years but no more than 80 years of age. Informed and written consent. Asymptomatic knees and no radiographic osteoarthritis.
Exclusion criteria	Patients with a thigh circumference exceeding 60 cm. Patients with conditions that severely compromise their gait other than knee osteoarthritis in the affected knee. Patients with previous severe fractures at the knee level or severe malalignment at the knee level. Surgically implanted metallic parts and pacemaker. Patients with need for an augmentation and/or stem extension. Patients who cannot perform the exercises.	Patients with a thigh circumference exceeding 60 cm. Patients with conditions that severely compromise their gait. Patients with previous fractures or severe malalignment at the knee level. Surgically implanted metallic parts and pacemaker. Patients who cannot perform the exercises.

Table I

Inclusion and exclusion criteria

	Healthy (n=15)	KOA patients (n=66)	G1 (n=20)	G2 (n=17)	G3 (b=10)	G4 (n=19)	P-value*	P-value**
a) Demographics with means and confidence intervals for continuous parameters and percentage for categorical parameters.								
Age	65.1 (60.1;70.1)	63.2 (61.1;65.2)	66.8 (64.2;69.4)^{G2}	57.5 (54.0;60.9)^{G1}	64.3 (56.3;72.3)	63.8 (59.8;67.9)	0.419	0.007
Side (left %)	46.7	54.6	45.0	76.5	30.0	57.9	0.581	0.131
Gender (female %)	26.7	39.4	40.0	41.2	20.0	47.4	0.348	0.536
Height	172.0 (167.3;176.7)	172.5 (170.9;174.6)	173.1 (169.3;176.9)	175.5 (172.4;178.5)	173.2 167.0;179.3)	169.3 (165.3;173.4)	0.794	0.236
Weight	78.1 (71.7;84.4)	86.5 (82.8;90.1)	87.75 (82.5;93.0)	88.3 (80.9;95.7)	81 (71.1;90.9)	86.3 (77.1;95.6)	0.044	0.211
Body Mass Index	26.2 (25.1;27.4)^{P}	29.0 (27.6;30.1)^{H}	29.3 (27.6;31.1)	28.7 (26.3;31.1)	26.8 (24.7;29.0)	30.0 (27.2;32.8)	0.001	0.075
Thigh circumference	51.5 (49.2;53.8)	52.1 (50.7;53.5)	51.9 (49.2;54.6)	53.3 (50.3;56.2)	50.2 (46.6;53.8)	52.2 (49.5;55.0)	0.711	0.700
b) Clinical characteristics with means and confidence intervals for continuous parameters and percentages for categorical parameters (except for the OA Ahlbeck score, which is presented with mean and confidence interval).								
ACL deficiency (0/1/2) %	73 / 27 / 0 $^{P, C2, C3}$	30 / 38 / 32^{H}	45 / 35 / 20^{C3}	24 / 41 / 35^{H}	**0 / 30 / 70$^{H, C1}$**	37 / 42 / 21	0.004	<0.001
PCL deficiency (%)	6.7	12.1	10.0	11.8	10.0	15.8	0.544	0.943
MCL deficiency (%)	0.0	7.6	0.0	5.9	0.0	21.5	0.271	0.174†
LCL deficiency (%)	6.8	6.1	5.0	11.8	0.0	5.3	0.930	0.866†
OA Ahlbeck grade	0.7 (0.3;1.0) $^{C1, C2, C3, C4}$	2.8 (2.5;3.1)	2.7 (2.4;3.0)$^{H, C3}$	2.2 (1.8;2.7)$^{H, C3}$	**3.9 (3.4;4.4)$^{H, C1, C2}$**	2.8 (2.2;3.4)^{H}	-†	<0.001
OA medial (%)	53.3	72.7	95.0^{C2}	29.4$^{C1, C4}$	60.0	94.7^{C2}	0.142	<0.001
OA lateral (%)	0.00	9.09	0.00	**35.29**	0.00	0.00	0.225	-†
OA medial+lateral (%)	6.7	16.7	5.0	29.4	40.0	5.3	0.970	0.029
FJS	98.6 (97.1;100.1)$^{P, C1, C2, C3, C4}$	16.0 (12.3;19.7)^{H}	15.3 (9.2;21.4)^{H}	12.3 (6.7;17.8)^{H}	20.0 (3.2;36.8)^{H}	17.9 (10.6;25.2)^{H}	<0.001	<0.001
OKS	47.8 (47.6;48.0)$^{P, C1, C2, C3, C4}$	23.5 (21.9;25.0)^{H}	23.15 (20.4;25.9)^{H}	23.4 (20.3;26.4)^{H}	22.5 (15.7;29.3)^{H}	24.5 (22.0;26.9)^{H}	<0.001	<0.001
KOOS SYMPTOMS	98.6 (97.1;100.0)$^{P, C1, C2, C3, C4}$	48.9 (44.6;53.2)^{H}	49.5 (40.5;58.4)^{H}	40.5 (33.7;47.4)^{H}	52.9 (39.3;66.4)^{H}	53.8 (45.5;62.0)^{H}	<0.001	<0.001
KOOS PAIN	99.6 (99.1;100.2)$^{P, C1, C2, C3, C4}$	43.5 (39.8;47.2)^{H}	39.4 (33.0;45.8)^{H}	42.6 (37.0;48.3)^{H}	46.4 (28.7;64.0)^{H}	46.9 (40.4;53.4)^{H}	<0.001	<0.001
KOOS ADL	99.7 (99.4;100.0)$^{P, C1, C2, C3, C4}$	51.5 (48.1;55.0)^{H}	49.1 (43.3;54.9)^{H}	49.4 (43.1;55.7)^{H}	56.6 (43.1;70.1)^{H}	53.3 (46.6;60.1)^{H}	<0.001	<0.001
KOOS SPORT/REC	96.3 (92.9;99.7)$^{P, C1, C2, C3, C4}$	15.1 (11.5;18.6)^{H}	13.8 (8.4;19.1)^{H}	15.9 (7.5;24.2)^{H}	15.0 (2.0;28.0)^{H}	15.8 (8.8;22.8)^{H}	<0.001	<0.001
KOOS QOL	97.9 (95.8;100.1)$^{P, C1, C2, C3, C4}$	27.4 (24.5;30.3)^{H}	23.4 (19.0;27.9)^{H}	28.3 (22.8;33.8)^{H}	28.1 (16.9;39.3)^{H}	30.3 (24.1;36.4)^{H}	<0.001	<0.001
VAS – gait	0.0 (0.0;0.0)$^{P, C1, C3, C4}$	2.4 (1.5;2.5)^{H}	2.9 (1.7;4.1)^{H}	1.5 (0.5;2.6)	2.3 (1.1;3.5)^{H}	2.9 (1.8;4.0)^{H}	<0.001	<0.001
OPR bilateral	0.0	9.9	15.0	5.9	30.0	5.3	0.156	0.242
c) Kinematic characteristics with overall difference when compared with the healthy group. The superimposed colour-squares, which are identical to those in Figure 6, highlight trajectories with similar differences when compared with the healthy control group.								
Flexion (+) / Extension (-)			**↑ Flexion (sections)**				-	-
Adduction (+) / Abduction (-)			↑ Adduction (full)	**↑ Abduction (full)**	↑ Adduction (full)	↑ Adduction (full)	-	-
Internal rotation (+) / External rotation (-)	↑ External (section)				↑ External (full)	↑ External (full)	-	-
Medial shift (+) / Lateral shift (-)	↑ Lateral (sections)				↑ Lateral (sections)	↑ Lateral (full)	-	-
Anterior drawer (+) / Anterior drawer (-)				↑ Anterior (sections)	**↑ Anterior (full)**	**No anterior**	-	-
Joint distraction (+) / Joint narrowing (-)	↑ Narrowing (full)	↑ Narrowing (full)	↑ Narrowing (full)	↑ Narrowing (full)	↑ Narrowing (full)	↑ Narrowing (full)	-	-

The superscript: H (the healthy group), P (the KOA-patient group) C1 (*the flexion group*), C2 (*the abduction group*), C3 (*the anterior drawer group*), and C4 (*the external rotation group*) show to which groups a significant difference was identified after Bonferroni adjustment.
The bold-cell data illustrate results of high importance.
*Comparison between the healthy group and the entire KOA patient group using either a t-test or a chi-squared test.
**Comparison between the healthy group and the clusters using either one-way analysis of variance, ordinal logistic regression or logistic regression.
†Statistical difference could not be estimated for groups without events.

Table II

Group summary and comparison

Osteoarthritis and Cartilage

Volumetric imaging

All participants underwent a computed tomography (CT) (Revolution EVO, GE Medical Systems, Milwaukee, WI, US) to construct subject-specific bone models (Fig. 3). A helical scan protocol with the reconstruction kernel 'boneplus' was used covering 15 cm of the most distal and proximal part of the femur and tibia. Knee scans were acquired with axial slices at a peak voltage of 100 kVp and 200 mAs, a slice thickness of 0.625 mm and a pixel spacing of 0.48×0.48 mm. The CT also included imaging with minor changes to reduce dose exposure of the femoral head (slice thickness of 2.5 mm) and ankle (80 kVp and slice thickness of 2.5 mm) to construct an anatomical coordinate system using the mechanical axis. Bones were segmented using an implemented, fully automated graph-cut segmentation method employing the Insight Segmentation and Registration Toolkit (Kitware, Clifton Park, NY, USA)[15,16]. From the segmentations, both three-dimensional volume and surface bone models were created. The volume model comprised the extracted bone containing the greyscale information of the CT. The surface model was extracted using the marching cubes algorithm and the visualization Toolkit (Kitware). An anatomical coordinate system was assigned to all bone models using a modified version of Miranda *et al.*[17] to implement the mechanical axis[11].

Analysis of dynamic radiographic imaging

The series of stereoradiographs were analyzed using an automated software system developed at our institution (AutoRSA software, Orthopaedic Research Unit, Aarhus, Denmark). The software utilized a digitally reconstructed radiographic (DRR) registration method to estimate bone pose from virtually generated projections using mathematical optimization algorithms, as previously described in more detail[13,16,18]. The optimal pose was found by minimizing the difference between virtually generated DRR images from a 3D volume to actual stereoradiographs using a normalized gradient correlation approach[13,18,19]. Prior to the DRR registration process, the automated bone pose initialization between frames deviated from previously described studies[13,16,18] by utilizing the skin-attached marker trajectories.

Quantification of knee joint kinematics

We implemented the joint coordinate system [Fig. 3(e)] initially defined by Grood and Suntay[20] to describe the knee joint kinematics, but using the modified equations proposed by Dabirrahmani and Hogg[21] to account for possible hyper-extension and hyper-flexion. The relative motion in all six degrees-of-freedom

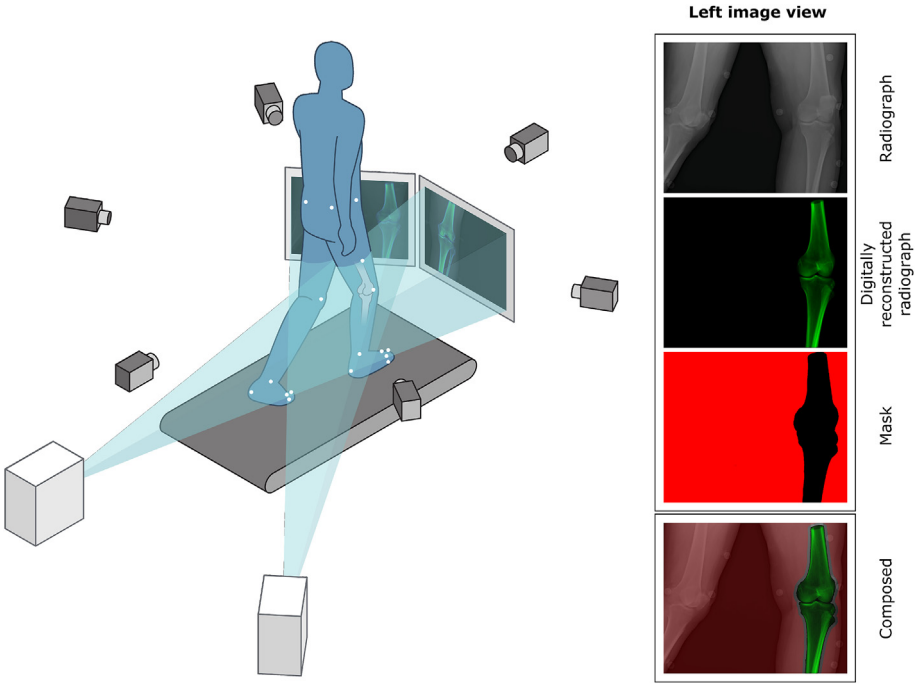

Fig. 1 Osteoarthritis and Cartilage

Illustration of the treadmill setup. Utilizing the largest recording area possible, we used a biplanar setup where the detectors were placed on individual stands with a relative angle of 40°; one in front of the subject and one to the side of the limb of interest. The source image distance was approximately 240 cm (frontal view) and 280 cm (side view). The source object distance was approximately 190 cm (frontal view) and 220 (side view). The system was acting in a plane parallel to the floor at a patient-specified height to centralize the knee joint in the radiographic images throughout the entire recording. The setup was mirrored for left/right knees to accommodate having the investigated knee as close as possible to the side view. The six optical cameras were positioned strategically surrounding the subject to avoid occluded markers during analysis of the skin-attached reflective markers. The markers (white dots) were attached at the subjects' pelvis, lower limb, and feet; three cluster markers at the thigh, two at the knee epicondyles, three cluster markers at the shank, two at the ankle malleolus, one at the heel, three at the metatarsales (1, 3, 5), and one at the first distal phalanx. The mask image was used for a refined optimization on each frame excluding irrelevant pixel values surrounding the DRR overlay image area of interest.

(rotation and translation) of the body-fixed anatomical coordinate systems was computed for each frame. The translation was quantified in mm with medial tibial shift, tibial anterior drawer, and joint distraction as positive directions. Rotations were measured in sequence as presented and quantified in degrees with flexion, adduction, and tibial internal rotation as positive directions. Kinematic values were divided into gait cycles, starting and ending with two successive initial foot contacts of the ipsilateral limb. We used the approach of O'Conner *et al.*[22] to identify initial contact using the optical markers on foot. To estimate each subjects' most representative gait cycle pattern, we time-normalized the kinematic measures to 21 points representing the gait cycle from 0 to 100% and calculated the median across trials for each subject.

Clinical characteristics

Based on conventional radiographs, KOA was classified according to the Ahlbeck score (grade 1–5). Those without KOA were classified as grade 0. Additionally, we registered the affected tibiofemoral compartment as lateral or/and medial. Knee ligament lesions were assessed with high accuracy and repeatability using detailed magnetic resonance imaging (1.5 T Avanto, SIEMENS, Erlangen, Forchheim, DE)[23]. We applied a modified version of the Osteoarthritis Initiative protocol[24] based on GE scanner recommendations (T2 SAG de3D DESS WE acquisition with 0.7 mm slice thickness and T1 COR fl3D WE with 1.5 mm slice thickness). We evaluated the following knee ligaments: ACL, posterior cruciate ligament (PCL), medial collateral ligament (MCL) and lateral collateral ligament (LCL). The ACL was graded as: 0 (no lesion), 1 (partial lesion), and 2 (full lesion). PCL, MCL, and LCL were registered as 0 (intact) or 1 (with lesion). The clinical outcome measures were assessed by the Oxford Knee Score (OKS), the Forgotten Joint Score (FJS) and the Knee Osteoarthritis Outcome Score (KOOS).

Subgroup allocation

The median kinematic trajectories of each patient were used to construct a 126 by 66 feature matrix (M) containing the 126 trajectory kinematic feature points (6 kinematic parameters × 21 time-points) for each of the 66 patients. Feature point ordering was consistent across all participants in the matrix. For the purpose of clustering, each feature was standardized to avoid different weightage between features. Each feature was subtracted by the respective mean values and divided by the standard deviation.

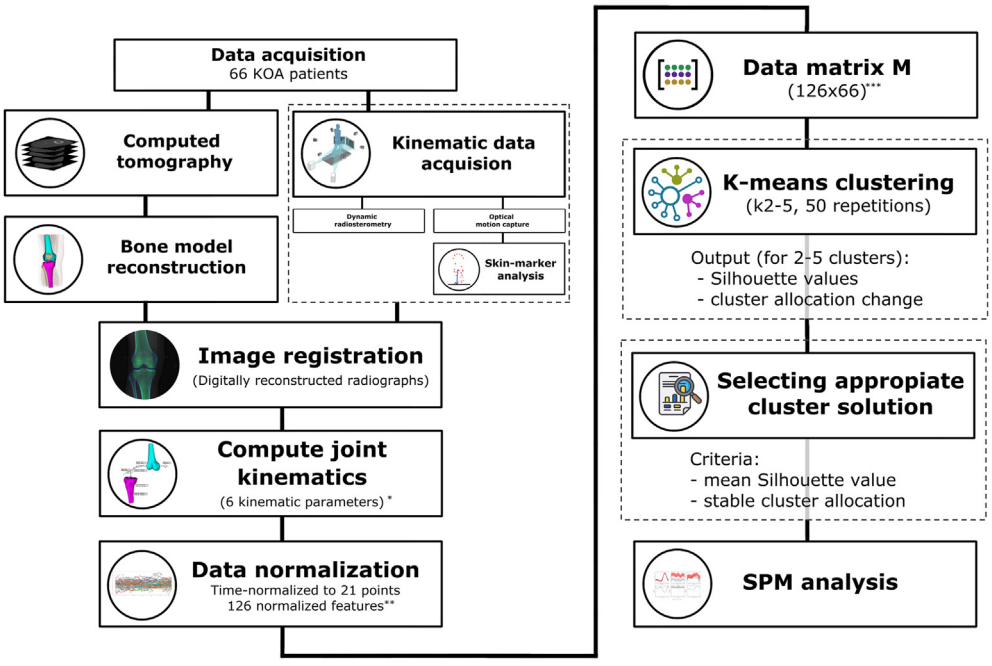

Fig. 2

Osteoarthritis and Cartilage

Illustration of the data analysis workflow. KOA – knee osteoarthritis, SPM – statistical parametric mapping. * The 6 kinematic parameters: flexion/extension, adduction/abduction, external/internal tibial rotation, lateral/medial tibial shift, anterior/posterior tibial translation, and joint distraction/narrowing. ** The 126 features (6 × 21) include the 6 kinematic parameters concatenated after time-normalization to 21 points representing the gait cycle from 0 to 100%. *** The data matrix M (126 × 66) were constructed of the 126 features (6 kinematic parameters × 21 time-points) and the 66 patients.

Subgroup allocation was performed with skleans[25] implementation of k-means clustering in Python. K-means clustering is an iterative algorithm randomly allocating every data point to the nearest subgroup, while minimizing the sum of squared Euclidian distance between every data point and its subgroup's centroid. Due to random seeding of the initial allocation, the k-means algorithm may not reach the global optimum, but instead converge to a local optimum. To handle this limitation, each clustering process was based on 50 repetitions with different, randomly allocated seeds. The repetition with the lowest sum of squared Euclidian distance was chosen as the final allocation of one *clustering process*. Another challenge of the k-means approach is to determine the number of subgroups, *k*. To do so, we investigated repeatability and quality for *k* number of subgroups ranging from two to five. Subgroup repeatability was evaluated based on repeating ten *clustering processes* for each of which we tracked differences in subgroup allocations with increasing *k*-subgroups. Subgroup quality of the two to five k-subgroups was assessed using the Silhouette value of the *clustering process* with the lowest sum of squared error of 10 repetitions (considered as the best). The Silhouette value is a measure of similarity describing how well subjects is allocated within a subgroup in relation to all other subgroups. The value ranges from −1 to 1 with a larger value indicating a stronger association with its allocated subgroup, whereas a more negative value indicates a stronger association with other subgroups. Of these four subgroup allocations, the one with the best repeatability and quality was used in the subsequent analysis.

Statistical analysis

Differences in knee joint kinematics across the entire gait cycles were examined using one-dimensional SPM with the open-source code spm1d (spm1d.org, v.0.4.2) for Python (Python Software Foundation, v.3.6). SPM allows for examining the entire one-dimensional time series of kinematic trajectories, avoiding selection bias and allowing for non-directed hypothesis testing instead of reducing the dataset to a certain observation or alternatively risking false hypothesis testing due to multiple repeated measurements[2,3]. SPM uses Gaussian random field theory to calculate the threshold that only the significance level of equivalently smooth Gaussian random fields would cross when the null hypothesis is true. QQ-plots revealed that our kinematic data were not normally distributed. Thus, we used statistical non-parametric mapping (SnPM), which deals with smoothness implicitly and estimates the test statistics through permutation[26]. First, a Hotelling test was implemented on the entire vector field. Then, the post-hoc Hotelling test was applied to each vector component if the vector field level reached statistical significance.

We compared demographically and clinically characteristic differences between groups using one-way analysis of variance (ANOVA) for continuous variables, ordinal logistic regression for categorical variables, and logistic regression for binary variables. When significant differences were detected, Bonferroni correction was applied for group differences. Visual inspection of QQ-plots verified normally distributed data.

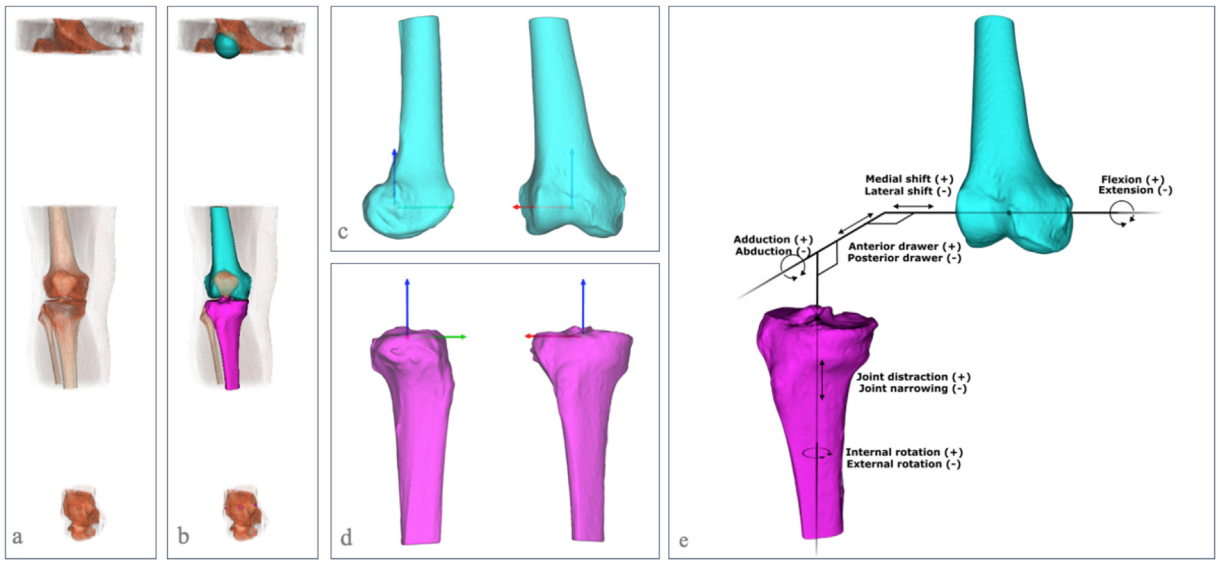

Fig. 3

Osteoarthritis and Cartilage

Illustration of the right leg of a CT (a), bone segmentation along with marked hip and ankle centres (b), anatomical coordinate system (c–d), and knee joint coordinate system (e). (a) Volume rendering of a hip-knee-ankle CT. (b) Bone segmentation of the femur (cyan) and tibia (magenta). The hip joint centre (cyan) was defined as the centre of a sphere fitted to the cortical bone of the femoral head using least square. The ankle centre (magenta) was defined as the midpoint between the ankle malleolus that was manually selected at the CT volume-rendered model. (c–d) 3D bone models of the femur (c) and tibia (d) bones in a sagittal and frontal view illustration the anatomical coordinate system. Femur: the lateral–medial axis was defined as the centre line of a cylinder placed using a least-square fit to the knee condyles, the proximal–distal axis was defined as an orthogonal projection from the medial–lateral axis to the centre of a sphere at the femoral head. The anterior-posterior axis was defined as the cross product of the medial–lateral axis and the proximal–distal axis. The origin was defined as the midpoint between the medial–lateral axis surface intersections. Tibia: the origin was defined as the centroid of the tibial plateau proximal of the largest cross section. The medial–lateral axis was defined as the first principal component axis. The proximal–distal axis was defined as an orthogonal projection from the medial–lateral axis to the midpoint between the ankle malleoli. The anterior-posterior axis was defined as the cross product of the medial–lateral axis and the proximal–distal axis. (e) Illustration of the knee joint coordinate system used for kinematic pose assessment of the femoral and tibial bones considered in relation to each.

Results

Subgroup allocation

The quality and repeatability analyses are presented in Fig. 4. Silhouette values [mean (standard deviation, SD)] across ten k-means cluster repetitions were: $k = 2$ [0.178 (0.002)]; $k = 3$ [0.140 (0.006)]; $k = 4$ [0.128 (0.004)]; and $k = 5$ [0.125 (0.005)]. The individual subgroup allocation across the ten consecutive repetitions showed identical subgroup allocation for $k = 2$. Individual data allocation was more variable for $k = 3$ and $k = 4$ with three and ten individuals switching subgroups, respectively. No consistent pattern of subgroup allocation could be identified for the $k = 5$ solution. Noticeably, the second ($k = 3$) and third ($k = 4$) solutions allocated two identical subgroups (G3,G4), whereas the third ($k = 4$) solution separated the remaining subgroup into two subgroups (G1,G2). All of this indicates that four subgroups may represent the optimal solution for separating the current dataset into the largest number of subgroups with the highest quality and reasonable repeatability. Consequently, the third ($k = 4$) solution was chosen for further analysis; G1 ($n = 20$), G2 ($n = 17$), G3 ($n = 10$), and G4 ($n = 19$).

Kinematic and clinical characteristics

The tibiofemoral joint kinematic trajectories for the entire patient cohort showed increased tibial external rotation, tibial lateral shift, and joint narrowing compared to the healthy group (Fig. 5). The four gait-trajectory-based subgroups (G1,G2,G3,G4) are compared to the healthy group in Fig. 6 and Table IIc (color-code highlight the main differences). The in-between subgroup kinematic comparison can be found in the Supplementary material. Clinical differences and a schematic overview of the most relevant differences between subgroups and the healthy control group are presented in Table II.

G1 – The flexion group

This was the only subgroup revealing different knee flexion when compared with the healthy group. Increased knee flexion was identified at initial contact, terminal stance, and terminal swing phase. Additionally, throughout the entire gait cycle, this subgroup showed greater adduction and joint narrowing than the healthy group. The clinical characteristics revealed that this subgroup consisted primarily of cases with medial tibiofemoral osteoarthritis. In relation to the other subgroups, this group displayed a

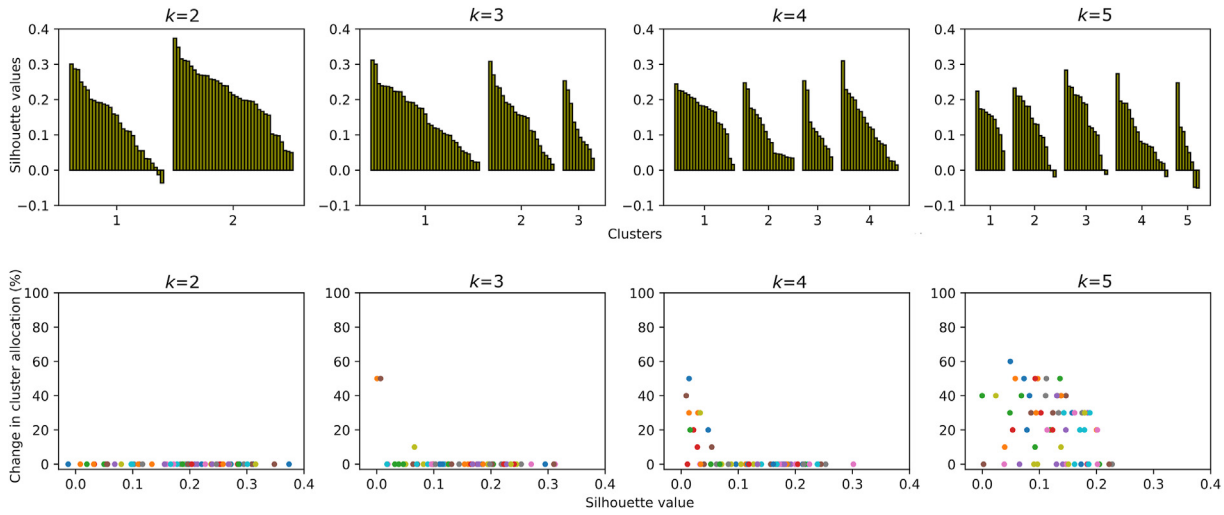

Fig. 4

Osteoarthritis and Cartilage

Presentation of cluster allocation for *k*-values ranging from 2 to 5. Top row: Silhouette values of each subject of the repetition that showed the best mean square error of the ten repetitions. Bottom row: Change in cluster allocation across the ten repetitions with respect to each subject's silhouette value.

larger flexion angle than *the anterior group* (loading response and initial swing phase) and *the external rotation group* (swing phase). Additionally, this subgroup displayed the largest internal rotation of any group.

G2 – The abduction group

This was the only subgroup revealing greater abduction than the healthy group. This was identified throughout the entire gait cycle. In addition, this subgroup showed greater joint narrowing throughout the gait cycle and anterior drawer during the loading response and terminal swing phase. The clinical characteristics revealed that it was the only subgroup that included cases with lateral tibiofemoral osteoarthritis. In relation to the other subgroups, this group displayed the largest abduction. In addition, it revealed a larger anterior drawer than *the flexion group* (stance, initial swing, and terminal swing) and *the external rotation group* (initial contact to mid-stance and terminal stance). It was only exceeded in this respect by *the anterior drawer group*.

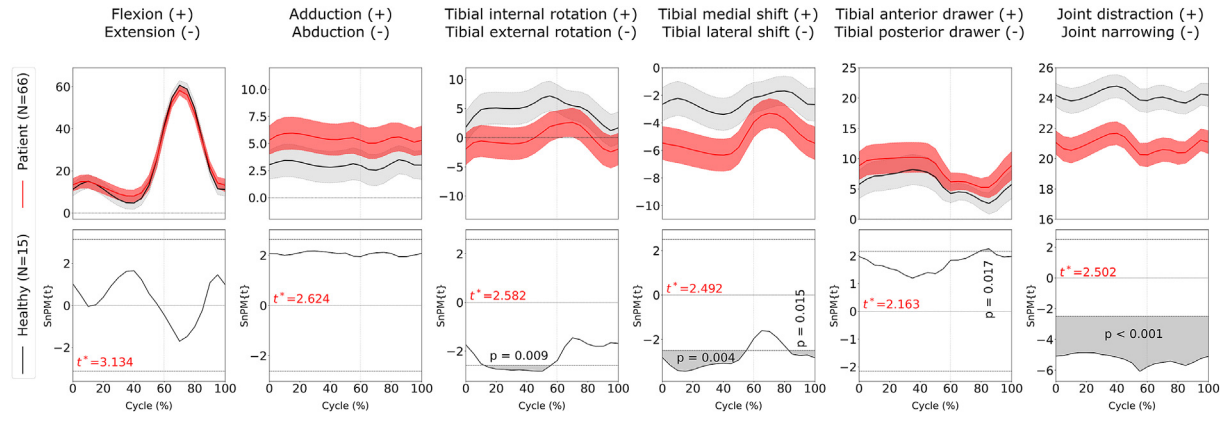

Fig. 5

Osteoarthritis and Cartilage

Kinematic comparison of the entire patient group with the healthy control group. The top row presents the mean trajectories of the two groups with confidence interval as the shaded area. The bottom row presents the ***post hoc*** non-parametric scalar field ***t*** tests (SnPM{t}), depicting where patients show higher (+) and lower (–) than healthy subjects. The thin dotted lines indicate the critical thresholds for significance. The grey-shaded areas illustrate when critical threshold is exceeded thus determining a significant difference.

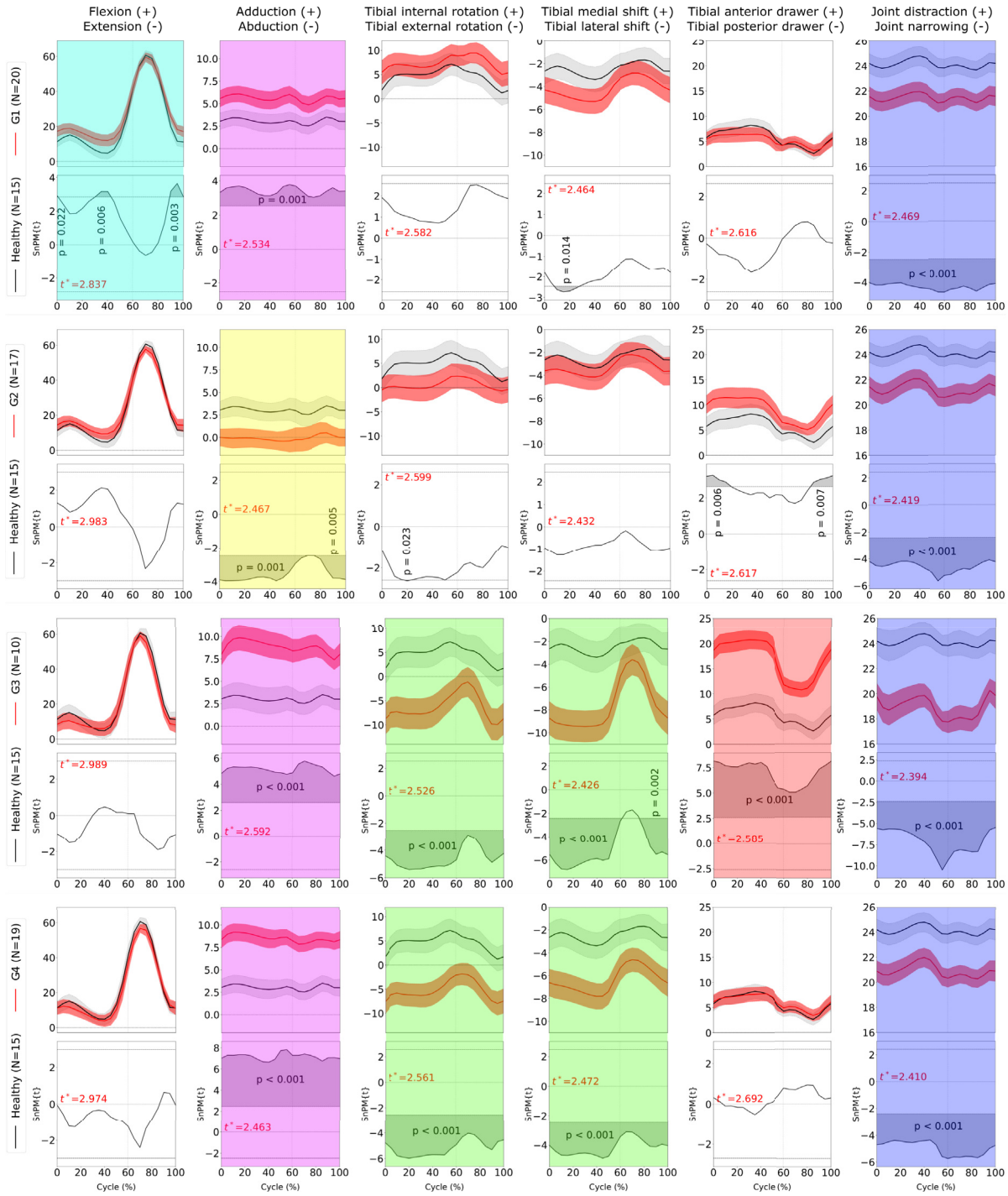

Fig. 6

Osteoarthritis and Cartilage

Statistical parametric mapping of all kinematic parameters (flexion/extension, adduction/abduction, internal/external tibial rotation, medial/lateral tibial shift, anterior/posterior tibial drawer, joint distraction/narrowing) for each cluster compared with the healthy control group. For each cluster comparison, the top row presents the mean trajectories of the two groups with confidence interval shown as the shaded area. The bottom row presents the ***post hoc*** non-parametric scalar field ***t*** tests (SnPM{t}), depicting where patients show more (+) and less (−) than healthy controls. The thin dotted lines indicate the critical thresholds of significance. The grey-shaded areas illustrate when the critical threshold exceeds; thus, a significant difference is present. The superimposed colour-squares highlight trajectories with similar differences when compared with the healthy control group: cyan presents increased flexion angle trajectories; magenta presents increased adduction angle trajectories; yellow presents abduction angle trajectories; green presents increased tibial external rotation and tibial lateral shift trajectories; red presents increased tibial anterior drawer; blue presents increased joint narrowing. The significance level was set to 5%.

G3 – The anterior drawer group

This was the only subgroup revealing severe anterior drawer throughout the gait cycle. Furthermore, this subgroup showed the largest external tibial rotation and lateral tibial shift throughout the motion (similar to G4) and larger adduction and joint narrowing compared with the healthy group. The clinical characteristics revealed that this subgroup was primarily composed of cases with medial tibiofemoral osteoarthritis, with partial and total ACL lesion and the largest KOA score of any group. In relation to the other subgroups, this group displayed the largest anterior drawer and, during the swing phase, the largest joint narrowing. In addition, like *the external rotation group,* it showed the largest adduction, external rotation, and tibial lateral shift. For this subgroup, increased lateral tibial shift was not observed during mid swing, whereas increased external rotation was not found during mid-swing, but this only applied when compared with *the abduction group*.

G4 – The external rotation group

This subgroup revealed, similar to G3, more external tibial rotation and lateral tibial shift, but no anterior drawer was observed compared with the healthy group. In addition, this subgroup showed more adduction and joint narrowing throughout the gait cycle. The clinical characteristics of this subgroup included the cases with the largest proportion of MCL and PCL lesions. In relation to the other subgroups, this group displayed, like *the anterior drawer group*, largest adduction, external rotation, and tibial lateral shift. For this subgroup, increased lateral shift was not observed during the swing phase compared with *the abduction group*, whereas increased external rotation was observed only when compared with *the abduction group*. Similar to lateral shift, no difference in external rotation was found during mid-swing between this subgroup and *the abduction group*.

All subgroups reported larger VAS pain scores during gait than the healthy group, with exception of *the abduction group* due to large variation in this group. However, no differences between subgroups were identified. Similarly, all subgroups had poorer clinical scores than the healthy group. Although the entire KOA patient group displayed greater Body Mass Index (BMI) than the healthy group and *the adduction group* included younger patients than *the flexion group* did, no other differences between groups were found in terms of potentially confounding variables (age, height, weight, side, and gender) (Table II).

Discussion

In patients with advanced KOA, we identified four clusters with homogeneous knee joint kinematics during gait that relate well with clinical characteristics but were clearly different from the knee joint kinematics of healthy volunteers without KOA. Our study differs from previous studies in three ways. First, we recorded the entire gait cycle using the accurate and precise dRSA method to assess knee kinematics (limits of agreement below 0.3° for rotation and 0.4 mm for translation)[13] rather than using traditional motion capture techniques that are often inhibited by soft-tissue artifacts. Second, we applied SPM, which allows examination of an entire kinematic trajectory thereby minimizing the risk of type-II errors and selection bias, which can be a problem with discrete-point comparisons. Third, we separated the patient cohort reversely by homogenous kinematics which present potential KOA phenotypes instead of applying the more often used predetermined clinical characteristics.

Previous gait studies of patients with KOA have compared various KOA group compositions to various control groups. KOA groups have been compared with healthy controls[4,27] and patients with medial tibiofemoral osteoarthritis have been compared with both healthy controls[5] and healthy controls with varus knee alignments[8]. Additionally, various discrete time-points and parameters during different gait phases have been used for group comparisons[4,5,8,27]. Thus, direct comparison with our results is challenging. However, a frequently chosen time point when comparing KOA and healthy groups is initial contact of the foot to the ground. At initial contact, diverse kinematic behaviors have been reported for patients with KOA compared with healthy controls: in patients with KOA, knee flexion has been identified as greater[5,27], lower[4], and similar[8] to that of healthy controls. Among these studies, three have investigated adduction and internal rotation. They found greater adduction[4,5,8], whereas the internal rotation showed both lower[4,5] and similar[8] rotations. Bytyqi *et al.*[8] and Zeng *et al.*[5] further investigated tibial anterior translation and found similar and lower translations, respectively. Only Zeng *et al.*[5] investigated the two remaining parameters, finding a greater tibial lateral shift and joint narrowing. The literature here presents various results based on various group comparisons. Thus, perhaps patients with KOA should not be assessed as a homogeneous group. Our results may explain this behavior and enhance our understanding of the KOA population as a heterogeneous group.

When comparing the entire KOA cohort with the healthy control group, we found increased tibial lateral shift, and joint narrowing at initial contact, whereas increased tibial external rotation first occurred later during stance. Thus, we cannot confirm the previous observations[4,5,8,28] which associate patients with KOAs with altered flexion, adduction, or anterior drawer. The likely reason for this is the large variation in kinematic trajectories in the KOA cohort. Thus, when the KOA cohort was clustered, we found statistically significant, clinically relevant differences for all kinematic parameters compared with the healthy control group. This suggests that the cohort of KOA patients comprises different kinematic phenotypes and that divergence in the results of previous investigations of the KOA group as a whole is due to the specific composition of kinematic subgroups included but not controlled for. This statement is substantiated by the fact that *the abduction group* (G2) was not observed until the number of subgroups increased from three to four. The identified kinematic characteristics of each subgroup could be linked to specific clinical characteristics. For example, *the flexion group* (G1), *the anterior drawer group* (G3), and *the external rotation group* (G4) revealed increased adduction. It displayed the largest portion of patients with medial tibiofemoral OA, whereas *the abduction group* (G2) revealed the largest proportion of patients with lateral tibiofemoral OA. Mechanically, this can be explained by the fact that reduced medial cartilage thickness increases a varus knee posture and, conversely, reduced lateral cartilage thickness increases a valgus knee posture[29]. Additionally, *the abduction group* (G2) and *the anterior drawer group* (G3) were the only subgroups revealing increased anterior drawer and larger ACL lesion grades than the healthy group. Additionally, *the anterior drawer group (G3)* showed the most prominent increase in anterior drawer and the largest proportion of patients with ACL rupture. Furthermore, *the anterior drawer group* (G3) also displayed the largest Ahlbeck score, representing a link between the well-established coherence of anterior-posterior knee instability and the development of KOA[30].

A systematic review[31] found that the course of pain and physical functioning in KOA were diverse and described a high heterogeneity across studies. The authors also suggested that KOA populations consist of subgroups or phenotypes. Our findings support this. However, the cluster scores and clinical outcome variables in our study indicate further subgroup overlap. Other subgroups and phenotypes have previously been identified. Knoop *et al.*[32] (later

confirmed by Holla *et al.*[33]) identified three subgroups with distinct trajectories of physical functioning over time (good, moderate, and poor). Esch *et al.*[34] identified five homogeneous clinical phenotypes (minimal joint disease phenotype, strong muscle strength phenotype, severe radiographic KOA phenotype, obese phenotype, and depressive mood phenotype). Another systematic review proposed six other phenotypes (chronic pain, inflammatory, metabolic syndrome, metabolic bone/cartilage, mechanical overload, and minimal joint disease). These phenotypes may potentially explain some of the variation in clinical outcomes within the identified subgroups in our study. Thus, further investigation is needed, including multiple characteristics, e.g., clinical, biomechanical, psychosocial, and genetic factors, categorizing and identifying phenotypes that embrace the heterogeneous pathology and multifactorial nature of patients with KOA.

Overall, TKA is a successful treatment for pain reduction in patients with KOA. However, up to 20% of treated patients are, dissatisfied with the outcome[35], and more than 50% have residual knee symptoms[36]. Although considerable effort has been devoted to increase patient satisfaction, this has not yet been accomplished. The natural knee joint is heterogenic in shape, size, and function. Gait kinematic phenotyping within KOA patients may help us better understand the contributory and persistent causes of TKA patients' dissatisfaction with outcomes. Maybe, various patient groups should undergo different interventions or treatment with specific implant designs. Treatment targeted more specifically towards selective phenotypes has also previously been suggested to lead to improved outcomes[37]. To clarify this, new research on the groups identified in this study needs to be conducted.

Some limitations of our study warrant discussion. First, the gait pattern on the treadmill may be different from that over ground. However, some reports have declared that only minimal differences in kinetic and kinematic parameters were found between treadmill and over-ground gait[38,39]. Barefoot walking may influence the load on the lower extremity joints within the subjects, but conditions were similar for the KOA group and the healthy group. Thus, we do not expect this to have influenced either the results or the conclusion. Second, inevitably, crossing leg coursed leg-projection overlap during dRSA acquisition. However, our setup ensured that one of the radiographic views were always free of overlay and we did not see a negative effect of leg-overlay on accuracy in the entire gait cycle. Third, the requirement of a maximum thigh circumference may have excluded obese subjects whom have showed altered kinematics.[40]

In conclusion, we found that patients with advanced KOA can be clustered into four subgroups based on homogeneous gait patterns. For these subgroups, we determined a meaningful relationship to different KOA-affected compartments, KOA progression and ligament lesions. A better understanding of knee joint pathomechanics in patients with KOA allows for phenotyping of subgroups, which may inspire improved and more patient-specific treatment strategies in the future.

Contributors

ETP was involved in all aspects of the study and drafted the manuscript. SR, DK, and JD operated the patients, whereas NEL and SR examined and labelled the clinical characteristics. SR, MSA and MS had an essential role in the study design, interpretation, and presentation of data. All authors contributed to data interpretation and manuscript revision.

Competing interest statement

The authors have no conflicts of interest to declare.

Acknowledgements

We thank for the financial support we received from: Aarhus University, The Danish Rheumatism Association, Toyota-Fonden, Købmand Sven Hansen og Hustru Ina Hansens Fond, and Søster og Verner Lipperts Fond. The study sponsors have no conflicts of interest to declare.

Supplementary data

Supplementary data to this article can be found online at https://doi.org/10.1016/j.joca.2021.10.011.

References

1. Davis MA, Ettinger WH, Neuhaus JM, Mallon KP. Knee osteoarthritis and physical functioning: evidence from the NHANES I epidemiologic followup study. J Rheumatol 1991;18(4):591–8.
2. Pataky TC. One-dimensional statistical parametric mapping in Python. Comput Methods Biomech Biomed Engin 2012;15(3):295–301, https://doi.org/10.1080/10255842.2010.527837.
3. Pataky TC, Robinson MA, Vanrenterghem J. Vector field statistical analysis of kinematic and force trajectories. J Biomech 2013;46(14):2394–401, https://doi.org/10.1016/j.jbiomech.2013.07.031.
4. Nagano Y, Naito K, Saho Y, Torii S, Ogata T, Nakazawa K, *et al.* Association between in vivo knee kinematics during gait and the severity of knee osteoarthritis. Knee 2012;19(5):628–32, https://doi.org/10.1016/j.knee.2011.11.002.
5. Zeng X, Ma L, Lin Z, Huang W, Huang Z, Zhang Y, *et al.* Relationship between Kellgren-Lawrence score and 3D kinematic gait analysis of patients with medial knee osteoarthritis using a new gait system. Sci Rep 2017;7(1):1–8, https://doi.org/10.1038/s41598-017-04390-5.
6. Zeni JA, Higginson JS. Differences in gait parameters between healthy subjects and persons with moderate and severe knee osteoarthritis: a result of altered walking speed? Clin Biomech 2009;24(4):372–8, https://doi.org/10.1016/j.clinbiomech.2009.02.001.
7. Farrokhi S, Tashman S, Gil AB, Klatt BA, Fitzgerald GK. Are the kinematics of the knee joint altered during the loading response phase of gait in individuals with concurrent knee osteoarthritis and complaints of joint instability? A dynamic stereo X-ray study. Clin Biomech 2012;27(4):384–9, https://doi.org/10.1016/j.clinbiomech.2011.10.009.
8. Bytyqi D, Shabani B, Lustig S, Cheze L, Karahoda Gjurgjeala N, Neyret P. Gait knee kinematic alterations in medial osteoarthritis: three dimensional assessment. Int Orthop 2014;38(6):1191–8, https://doi.org/10.1007/s00264-014-2312-3.
9. Na A, Piva SR, Buchanan TS. Influences of knee osteoarthritis and walking difficulty on knee kinematics and kinetics. Gait Posture 2018;61:439–44, https://doi.org/10.1016/j.gaitpost.2018.01.025.
10. Kuntze G, Nettel-Aguirre A, Ursulak G, Robu I, Bowal N, Goldstein S, *et al.* Multi-joint gait clustering for children and youth with diplegic cerebral palsy. PLoS One 2018;13(10), https://doi.org/10.1371/journal.pone.0205174.
11. Nielsen ET, Stentz-Olesen K, de Raedt S, Jørgensen PB, Sørensen OG, Kaptein B, *et al.* Influence of the anterolateral ligament on knee laxity: a biomechanical cadaveric study measuring knee kinematics in 6 degrees of freedom using dynamic radiostereometric analysis. Orthop J Sport Med 2018;6(8), https://doi.org/10.1177/2325967118789699.

12. Gray HA, Guan S, Thomeer LT, Schache AG, de Steiger R, Pandy MG. Three-dimensional motion of the knee-joint complex during normal walking revealed by mobile biplane x-ray imaging. J Orthop Res 2019;37(3):615–30, https://doi.org/10.1002/jor.24226.
13. Christensen R, Petersen ET, Jürgens-Lahnstein J, Rytter S, Lindgren L, De Raedt S, *et al*. Assessment of knee kinematics with dynamic radiostereometry: validation of an automated model-based method of analysis using bone models. J Orthop Res 2020, https://doi.org/10.1002/jor.24875. Published online.
14. Bohannon RW, Williams Andrews A. Normal walking speed: a descriptive meta-analysis. Physiotherapy 2011;97(3):182–9, https://doi.org/10.1016/j.physio.2010.12.004.
15. Krčah M, Székely G, Blanc R. Fully automatic and fast segmentation of the femur bone from 3D-CT images with no shape prior. Proc - Int Symp Biomed Imaging 2011:2087–90, https://doi.org/10.1109/ISBI.2011.5872823. Published online.
16. Hemmingsen CK, Thillemann TM, Elmengaard B, de Raedt S, Nielsen ET, Mosegaard SB, *et al*. Elbow biomechanics, radiocapitellar joint pressure, and interosseous membrane strain before and after radial head arthroplasty. J Orthop Res 2020;38(3):510–22, https://doi.org/10.1002/jor.24488.
17. Miranda DL, Rainbow MJ, Leventhal EL, Crisco JJ, Fleming BC. Automatic determination of anatomical coordinate systems for three-dimensional bone models of the isolated human knee. J Biomech 2010;43(8):1623–6, https://doi.org/10.1016/j.jbiomech.2010.01.036.
18. Hansen L, De Raedt S, Jørgensen PB, Mygind-Klavsen B, Kaptein B, Stilling M. Marker free model-based radiostereometric analysis for evaluation of hip joint kinematics. Bone Joint Res 2018;7(6):379–87, https://doi.org/10.1302/2046-3758.76.BJR-2017-0268.R1.
19. van der Bom IMJ, Klein S, Staring M, Homan R, Bartels LW, Pluim JPW. Evaluation of optimization methods for intensity-based 2D-3D registration in x-ray guided interventions. In: Dawant BM, Haynor DR, Eds. Medical Imaging 2011: Image Processing. SPIE; 2011:657–71, https://doi.org/10.1117/12.877655.
20. Grood ES, Suntay WJ. A joint coordinate system for the clinical description of three-dimensional motions: application to the knee. J Biomech Eng 1983;105(2):136–44, http://www.ncbi.nlm.nih.gov/pubmed/6865355. Accessed July 31, 2015.
21. Dabirrahmani D, Hogg M. Modification of the Grood and Suntay joint coordinate system equations for knee joint flexion. Med Eng Phys 2017;39:113–6, https://doi.org/10.1016/j.medengphy.2016.10.006.
22. O'Connor CM, Thorpe SK, O'Malley MJ, Vaughan CL. Automatic detection of gait events using kinematic data. Gait Posture 2007;25(3):469–74, https://doi.org/10.1016/j.gaitpost.2006.05.016.
23. Koch JEJ, Ben-Elyahu R, Khateeb B, Ringart M, Nyska M, Ohana N, *et al*. Accuracy measures of 1.5-tesla MRI for the diagnosis of ACL, meniscus and articular knee cartilage damage and characteristics of false negative lesions: a level III prognostic study. BMC Musculoskelet Disord 2021;22(1), https://doi.org/10.1186/s12891-021-04011-3.
24. Peterfy CG, Schneider E, Nevitt M. The osteoarthritis initiative: report on the design rationale for the magnetic resonance imaging protocol for the knee. Osteoarthritis Cartilage 2008;16(12):1433–41, https://doi.org/10.1016/j.joca.2008.06.016.
25. Pedregosa F, Varoquaux G, Gramfort A, Michel V, Thirion B, Grisel O, *et al*. In: Scikit-Learn: Machine Learning in Python 2011;vol. 12, http://scikit-learn.sourceforge.net.
26. Nichols TE, Holmes AP. Nonparametric Permutation Tests for Functional Neuroimaging: A Primer with Examples. Published online 2001, https://doi.org/10.1002/hbm.1058.
27. Favre J, Jolles BM. Gait analysis of patients with knee osteoarthritis highlights a pathological mechanical pathway and provides a basis for therapeutic interventions. EFORT Open Rev 2016;1(10):368–74, https://doi.org/10.1302/2058-5241.1.000051.
28. Heiden TL, Lloyd DG, Ackland TR. Knee joint kinematics, kinetics and muscle co-contraction in knee osteoarthritis patient gait. Clin Biomech 2009;24(10):833–41, https://doi.org/10.1016/j.clinbiomech.2009.08.005.
29. Eckstein F, Wirth W, Hudelmaier M, Stein V, Lengfelder V, Cahue S, *et al*. Patterns of femorotibial cartilage loss in knees with neutral, varus, and valgus alignment. Arthritis Care Res 2008;59(11):1563–70, https://doi.org/10.1002/art.24208.
30. Wallace DT, Riches PE, Picard F. The assessment of instability in the osteoarthritic knee. EFORT Open Rev 2019;4(3):70–6, https://doi.org/10.1302/2058-5241.4.170079.
31. De Rooij M, Van Der Leeden M, Heymans MW, Holla JFM, Häkkinen A, Lems WF, *et al*. Prognosis of pain and physical functioning in patients with knee osteoarthritis: a systematic review and meta-analysis. Arthritis Care Res 2016;68(4):481–92, https://doi.org/10.1002/acr.22693.
32. Knoop J, Van Der Leeden M, Thorstensson CA, Roorda LD, Lems WF, Knol DL, *et al*. Identification of phenotypes with different clinical outcomes in knee osteoarthritis: data from the osteoarthritis initiative. Arthritis Care Res 2011;63(11):1535–42, https://doi.org/10.1002/acr.20571.
33. Holla JFM, Van Der Leeden M, Heymans MW, Roorda LD, Bierma-Zeinstra SMA, Boers M, *et al*. Three trajectories of activity limitations in early symptomatic knee osteoarthritis: a 5-year follow-up study. Ann Rheum Dis 2014;73(7):1369–75, https://doi.org/10.1136/annrheumdis-2012-202984.
34. Van der Esch M, Knoop J, van der Leeden M, Roorda LD, Lems WF, Knol DL, *et al*. Clinical phenotypes in patients with knee osteoarthritis: a study in the Amsterdam osteoarthritis cohort. Osteoarthritis Cartilage 2015;23(4):544–9, https://doi.org/10.1016/j.joca.2015.01.006.
35. Bourne RB, Chesworth BM, Davis AM, Mahomed NN, Charron KDJJ. Patient satisfaction after total knee arthroplasty: who is satisfied and who is not? Clin Orthop Relat Res 2010;468(1):57–63, https://doi.org/10.1007/s11999-009-1119-9.
36. Nam D, Nunley RM, Barrack RL. Patient dissatisfaction following total knee replacement: a growing concern? Bone Jt J 2014;96B(11):96–100, https://doi.org/10.1302/0301-620X.96B11.34152.
37. Bijlsma JWJ, Berenbaum F, Lafeber FPJG. In: Arthritis 1 Osteoarthritis: An Update with Relevance for Clinical Practice 2011;vol. 377, www.thelancet.com.
38. Riley PO, Paolini G, Della Croce U, Paylo KW, Kerrigan DC. A kinematic and kinetic comparison of overground and treadmill walking in healthy subjects. Gait Posture 2007;26(1):17–24, https://doi.org/10.1016/j.gaitpost.2006.07.003.
39. Levine D, Richards J, Whittle MW. Whittle's Gait Analysis 2012.
40. Li J, Tsai T, Brentzel K, Ahn YJ, Felson DT. Three-dimensional knee joint kinematics in obese individuals with knee pain during treadmill gait. PLos One 2017;12(3):1–11, https://doi.org/10.1371/journal.pone.0174663.